SINGLE PHOTON EMISSION COMPUTED TOMOGRAPHY

A senior paper submitted in partial fulfillment of the requirement

For the degree of Bachelor of Science in

Physics from the College of William and Mary in Virginia

By

Kevin Christopher Knott

_____

Dr. Robert E. Welsh, Director

_____

Dr. Keith Griffioen

Williamsburg, Virginia

March 2001

TABLE OF CONTENTS

ABSTRACT

The goal of this project is to improve upon the current imaging system being used for real-time *in vivo* imaging of small animals. The system now in use was designed for detecting photons from and generating high-resolution planar images of the distribution of an injected radiopharmaceutical, iodine-125, which serves as a tag to trace other biochemical compounds of interest (Weisenberger 1998). Specific to our recent project, a gamma camera has been utilized to take 360° snapshot, planar projections of a phantom in order to detect the radiant photons emitted by the injected isotope of iodine. Computed tomography is then utilized to reconstruct sliced images of the distribution of radioactivity detected from the phantom. The major goal of this process, Single Photon Emission Computed Tomography, or SPECT, is to accurately locate the injected compound labeled by the radiotracer, iodine-125. It will be the purpose of this paper to outline and elaborate upon the principles behind this technique of Single Photon Emission Computed Tomography, as related and applicable to small animal imaging for this research in the future.

I. BACKGROUND

A. *Computed Tomography (CT)*

Since Godfrey N. Hounsfield developed the first clinical machine designed specifically for computed tomography (CT) in 1971, several different types of CT have been advanced for use in nuclear medicine and biomedical studies (Shepp 1983). X-ray CT has seen the most rapid advances in this field. Yet, other techniques such as SPECT and Positron Emission Tomography, or PET, are gradually gathering larger interest in nuclear medicine research.

The rapid growth seen in all forms of CT can be attributed mainly to the growing availability of more sophisticated computers capable of such a technique. For conventional nuclear medical imaging, the use of computers was helpful for enhancing the display quality of already acquired images or allowing the tracking of time-dependent phenomena, but computer techniques were by no means necessary for acquiring a pictorial output of information (Wolbarst 1993). With the advent of computed tomography, though, the computer has become absolutely essential for the reconstruction of images from raw data. In addition to the capacity for acquiring and storing large amounts of data, the computer must be capable of providing a simple and straightforward means of analysis of these acquired data. With more detailed and user-friendly computer software programs, programming the necessary calculations and displaying the resulting information have become far easier than that encountered in previously existing imaging applications.

Still, computed tomography, overall, is a far from simple technique. The basic aim is to compute the cross-sectional distribution of some physical property of an object

from projections or views taken from a number of different directions (Pullan 1981). Mathematically, let f(x,y) represent the cross-sectional distribution of the physical property of interest; it is a slice of the object, as depicted in Figure 1 below. The goal of CT is to reproduce as accurately as possible the function f(x,y). As an example, for both PET and SPECT, the function f to be reproduced represents the concentration of a radiopharmaceutical, or radioactive tracer, within the body (Hobbie 1997). For X-ray CT, the function f(x,y) to be reconstructed via tomography is the attenuation of photons in the X-ray beam upon detection (1997).

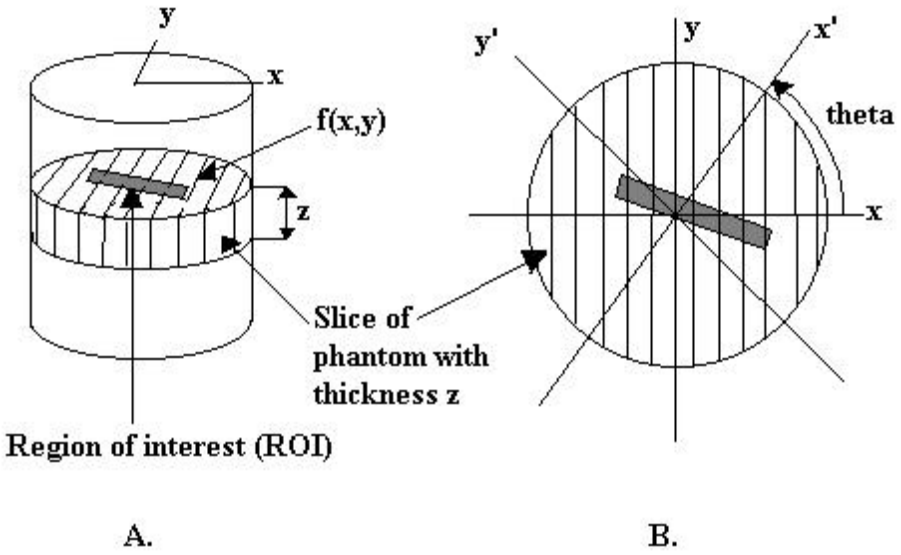

Figure 1 - The formation of projections of an object using computed tomography. A.) A phantom, which is an object used to simulate patient studies, illustrates the idea of a slice of an object, defined as f(x,y), with a uniform thickness z. B.) An overhead view of the slice of the object. The axes have been rotated through an angle theta to allow for an additional projection of the region of interest. A number of these views must be accumulated in a typical study of computed tomography (Pullan1981).

In all forms of tomography, a detector first measures the integral of f(x,y) along a line of emitted radiation. Rotating the (x,y) axes by an angle θ defines a new set of axes (x′,y′). Rotation of the axes is accomplished by either rotating the detectors around the

object or by rotating the object in front of the detectors in fixed integer units of θ. The detector output for each rotational angle will then be the integral of f(x′,y′), which is a projection of the function f(x,y) with the new set of axes. The line integral along this line, which is parallel to the y′-axis at a distance x′ from the origin, is known as the Radon transform (Cho 1993). By acquiring a sufficient set of projections taken at different angles θ and by analysis on a computer, the function f(x,y) can be determined and reconstructed. The determination of f(x,y) provides a two-dimensional slice of the object being imaged that has a constant, predetermined value of z. Stacking the constant z slices together reconstructs the three-dimensional distribution of the physical property under study. This reconstruction is the goal and final output of computed tomography.

In computed tomography, then, we are imaging slices of the object only so we can later reconstruct these slices into a united whole again. The reasoning behind such a backwards approach is not obvious. What the researcher performing this technique is hoping to acquire, though, is a clear image of the region of interest (ROI) in the object. In initial medical imaging techniques, subtle irregularities cropped up when trying to map the three dimensional object directly into two dimensions. The confusion arose because overlying structures could not be differentiated in the images. Lesions in the lung might be obscured by variations in the overlying ribs, for instance.

The methodology behind computed tomography is an attempt to solve this problem. CT's basis, then, is simply to mask out or ignore superfluous information in the whole image so that the researcher is viewing only that aspect of the object that is of particular concern to the study. In other words, by eliminating overlapping tissues and

structures that are unavoidably present in three dimensions, computed tomography achieves clarity of imaging by mapping the radiation into two dimensions.

It is not a direct mapping like past imaging studies, however. The mapping involves partitioning each slice under examination into a square matrix of thousands of small tissue volume elements, or voxels. The matrix carries a dimension depending on the number of voxels. For example, we have 128 x 128 matrices full of 128 volume elements in each direction, x and y. The image reconstruction process involves the determination of the value of f(x,y) of each voxel for each slice. The computed map of f is then displayed as a matrix of pixels in a two dimensional image, where each pixel displays the information from its corresponding voxel. The pixel display is the 2-D reconstructed image of the distribution of f(x,y).

To sum up the technique itself and its motivation in a more compact definition, *computed tomography* is a means of reconstructing an image of an object that clearly presents the features in the plane of interest without the confusion resulting from overlying structures that would be seen in images of the object as a whole (Pullan 1981). As already noted, there are many distinct applications of this technique, and each has a varying level of success as a nuclear imaging modality. For this reason, I will discuss briefly only two of the most successful and prominent, x-ray computed tomography and positron emission tomography, as an introduction and comparison to the topic of this paper, single photon emission computed tomography, or SPECT.

B. *X-ray Computed Tomography*

Most of the preliminary work in computed tomography was geared toward studies in X-ray CT, as computed tomography's inventor, Godfrey Hounsfield, originally applied his CT scanner to X-ray imaging. In X-ray computed tomography, sometimes called radiography, a patient is kept stationary while a detector and X-ray tube rotate around the patient, stopping at fixed positions while a beam of X-rays is emitted from the source, collimated, and sent through the patient into a detector. The X-ray photons are collimated to illuminate only that part of the subject of interest to the study (Hobbie 1997).

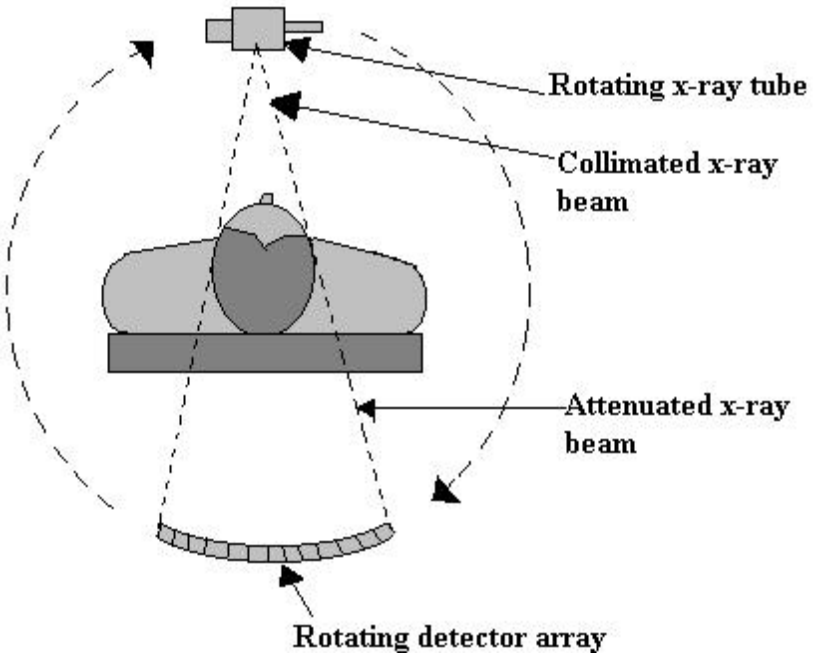

Figure 2 - Typical X-ray CT detection set-up. The x-ray tube and detectors rotate around the patient. The detectors, which are interfaced with a computer network, allow for a two-dimensional image of the detected x-rays to be produced on a monitor. This image is processed further to create slices of the imaged x-rays. The slices can be reconstructed to show the three-dimensional differentiation of x-ray attenuation.

In Figure 2, the detector is used to record a two-dimensional image of the patient's body. A number of these different angular views are accumulated by rotating the x-ray tube and the detectors around the body. A computer program is then utilized to reconstruct slices of the subject. As the name *tomography* (literally picture of a slice) suggests, the initial display of the reconstruction is just a single slice of the object carrying a constant value of z (Herman 1980). The computer program can be used again to stack each slice together in the proper sequence, thus reconstructing the 3-dimensional distribution of X-ray densities detected by the system after passing through the patient.

This method's principle motivation is that attenuation will result in the X-ray beam due to both absorption and scattering by the patient's tissue (Chandra 1976). By measuring only those photons that remain in the unscattered, or transmitted, beam the loss of photons can be measured. It is this loss of photons in the detected beam that we call the attenuation. Only photons that have not interacted in the material remain in the beam. So, by calculating the loss of photons in the beam, or attenuation, it is possible to reveal spatial variations in the detected X-ray densities (Robb 1995). To the extent that the various tissues of interest have differences in X-ray attenuation, the different spatial densities of X-rays detected are directly used to differentiate different tissues of interest. X-ray CT has proved particularly useful in detecting the location of tumors, where the differentiation in tissue is made between healthy tissue and that of the tumor (Herman 1980).

C. *Positron Emission Tomography (PET)*

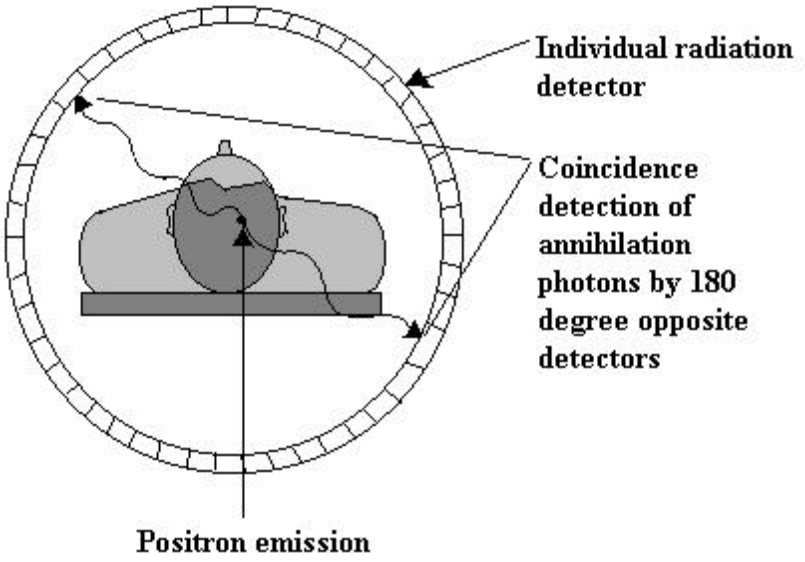

Figure 3 - A typical positron emission radiation detector. After decay of the radioisotope within the body, 180-degree opposite detectors record the annihilation photons in coincidence only if they are detected simultaneously; a process known as "electronic collimation."

A second method of computed tomography, not as commonly known or widely used as X-ray CT, is positron emission tomography, or PET. This technique is used to acquire 3-dimensional information regarding the biological distribution of a radiopharmaceutical. A typical positron emission detector set-up is pictured above in Figure 3. The basic process is as follows: 1. A radioactive tracer is produced by some form of accelerator (i.e. a cyclotron) and injected into the body. 2. The radioisotope decays by a process called positron emission, or ß+ emission. 3. The positron annihilates upon collision with an electron in matter (the subject's body). 4. The annihilation releases energy and results in the conversion of the electron and positron into a pair of 511 keV gamma rays travelling colinearly in opposite directions. 5. The two gamma rays, travelling at 180° opposite directions, are detected in coincidence. 6.

Coincidence detection is made possible by a coincidence detection circuit, which only records an event if both detectors sense annihilation photons simultaneously. 7. Tomographic techniques analyze this detection to yield images of the distribution of positron-emitting radiotracers administered to the subject (Weisenberger 1998).

Every system has both efficient and inefficient uses and characteristics that consequently render the system suitable for particular studies and not suitable for others. For instance, the usefulness of positron emission tomography depends heavily on three general factors. One must first consider the characteristics of the radiopharmaceuticals that will be used in the study. They have a very short lifetime, and so require a nearby cyclotron for production and prompt delivery. A careful look must also be given to the efficiency of the method of collimation. A collimator is used in PET applications to reduce the amount of scattering photons detected. Lastly, a merit of PET worth consideration is the particular ease with which it lends itself to tomographic imaging.

First and foremost concerning the characteristics of the radiopharmaceutical, most cameras being used currently in nuclear medicine studies are not well suited for imaging annihilation photons. This is a distinct disadvantage of PET. To complicate matters further, the total number of radionuclides that decay by positron emission and that are applicable to biological studies is relatively small; and, those that do decay by ß+ emission have very short half-lives (^{11}C = 20 min.; ^{13}N = 10 min; ^{15}O = 2 min; ^{18}F = 110 min). Such short half-lives require an accelerator to be present at the site, which is both expensive and impracticable for most uses of PET (Hobbie 1997). Yet, as a consequence and benefit of their short half-lives, the radionuclides used in PET applications allow imaging with minimal radiation dosages to patients. This is an extremely important

consideration, and it may outweigh the price of cyclotron production, depending on the application at hand. If cyclotron production is affordable, limiting radiation exposure to the patient is a large advantage over SPECT studies. Additionally, it should be noted that although the number of radionuclides decaying by PET-usable emissions is small, the ones that do are extremely useful. ^{11}C, ^{13}N, and ^{15}O are the three major components of molecules in living matter. This is an especially important point since most applications of PET are concerned with the relationship of the radionuclides with the metabolic processes in animal physiology (Cho 1993).

An added concern of PET studies is the issue of collimation. A large amount of collimating material, typically lead or tungsten, is necessary to absorb the high-energy annihilating photons. This proves drastically inefficient in most cases because it necessitates the construction of massive detector systems, which increases expenses and time (Robb 1995). Sidestepping this problem, though, one notices that positron emission tomography uses coincidence detection to record annihilation photons. Because of the simultaneous detection of these photons along the colinear column or strip joining the two detectors, coincidence detection can be used as a means of collimation. For this reason, coincidence detection in PET is also called "electronic collimation" (Cho 1993). Electronic collimation eliminates the problem of unnecessarily large detector systems, and due to the fact that detector sensitivity is dependent on collimator thickness, the lack of external collimator material increases the possible sensitivity (photon collection capability) of the detector system. A higher level of maximum photon sensitivity can also be viewed as an additional advantage of PET over SPECT, but the necessary circuitry for PET is usually more intricate and expensive.

A third factor concerning the process of positron emission tomography is a more general feature of the technique. The detector set-up lends itself particularly well to the reconstruction of images from projections via computed tomography. This characteristic of PET also owes its merit to the detection of the annihilation photons in coincidence. The accuracy of the spatial resolution achievable by this detection is limited only by the physical properties of the annihilation, and not by any collimation limitations. This sets the lower limit of spatial resolution at about 2-3 mm fwhm, equaling (and in some cases bettering) most other tomographic imaging modalities.

D. *Single Photon Emission Computed Tomography (SPECT)*

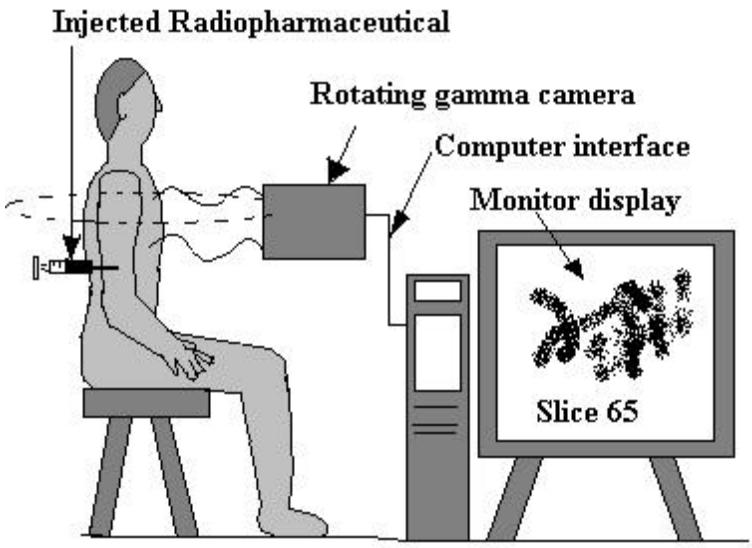

Figure 4 - A SPECT application. A gamma camera is used to rotate fully around the patient. It detects the radiant gamma ray photons emitted by the injected isotope. A computer is then utilized to form sliced images of the emitted radiation.

The third method of computed tomography that is gathering potential as a means of biomedical study is that of Single Photon Emission Computed Tomography, or

SPECT. It is the goal of this paper to elaborate further upon the particular detector set-up that has been developed here at William and Mary and which is capable of producing SPECT images. But, first I will detail some of the motivations behind the technique and give a brief outline of the process and goals of our study.

Similar to positron emission tomography, SPECT is a high-resolution means of reconstructing a distributive map of the concentration of a radioactive tracer (this will be elaborated upon in the introduction to SPECT). The radiopharmaceutical in this case is also injected into the patient, but the means of production does not require a cyclotron. The radioactive isotope decays within the patient, and the detector (gamma camera) is capable of detecting these decays. Figure 4 on the previous page illustrates a typical SPECT application in which the isotope is injected, decays, and is detected by the gamma camera. Similar to the method of x-ray CT, a computer is used to accumulate separate views of the radiation and recreate sliced images of the object.

The principle advantage of such a nuclear medicine imaging system, as recognized today, is to provide functional information that is generally difficult or impossible to obtain via other imaging techniques. Functional information is the information that is obtained as the radiopharmaceutical comes into contact with the anatomical structure of the animal *in vivo*. Without a doubt, SPECT has found more widespread use today for this reason. It is a unique way to non-intrusively show various biochemical functions in live animals (Cho 1993). Unlike X-ray CT, for instance, SPECT can show the increase and decrease of activity in a particular area of a mouse brain as the radiopharmaceutical passes through the mouse's system *in vivo*.

It is this application that the detector system currently being utilized for phantom studies in our laboratory hopes to implement in the future. Particularly, we are attempting to use SPECT images to study the biological processes within mice. We will focus on obtaining a greater understanding of mechanisms of gene expression, and on questions within the diabetes field. This form of research uses a specific tracer molecule to bind to target molecules, which can allow a study of specific genes and their expression (Weisenberger 1998). Tracer molecules, such as probes and ligands, are utilized for their ability to bind to specific target RNA molecules and proteins, respectively. The location of binding is entirely determined by the physiological response of the animal to the tracer compound. In the future, normal and diabetic mouse studies will be used to compare binding locations for the probes and ligands of interest. The comparable differences in binding locations should then shed some light on the differences between normal and diabetic mice.

Yet, before we can achieve these goals, there are initial steps that have to be taken to ensure that the results we find with animals in the future are useful. The means to achieving these goals first rests in the calibration and testing of our detector system and our SPECT software. We currently use a SPECT phantom to accumulate data and run our software. This limits the number of mice that will have to be used in research, and it allows us to determine the best possible resolution and sensitivity achievable by the detector system.

II. SPECT

A. *SPECT Summary*

The basic process of SPECT as performed in our laboratory is as follows: A gamma camera is utilized to take snap-shots of the SPECT phantom and to detect the distribution of radiation/photons emitted by the injected radioactive substance of choice (in our case, iodine-125, which emits X-rays and gamma ray radiation). A scintillator first converts the collimated photons from the radioactivity into visible light. The visible light is then detected by a position sensitive photomultiplier tube (PSPMT), which emits electrons via the photoelectric effect.

The emitted electrons are intercepted by the crossed wire anodes of our PSPMT, and the anode output signals are then fed into analog-to-digital-converter cards, converting the amplitude of the PSPMT signal into a number that can be stored and analyzed by our computer system. The data acquisition software acquires a real-time planar image by displaying these position-sensitive digital output signals. Rotating the phantom in front of the camera allows a number of incremental angular views to be accumulated, stepping through from 0° to 360°. Each angular view is saved, filed, and run through a SPECT computer program that forms slices of the object being studied. These slices are then displayed to give a two dimensional image of the reconstructed distribution of radioactivity in the body.

B. *Radioactivity/Iodine-125*

The goal of SPECT nuclear medicine techniques is to provide information on the distribution of administered radiopharmaceuticals. The radiopharmaceutical consists of a

pharmacologic agent, i.e. a probe or ligand, which is used to biologically interact with the subject, and a radioactive tag, which is used to trace the distribution of the agent under study (Wolbarst 1993). Such research exploits the tendency of certain tagged agents to concentrate in specific organs or biological compartments within the subject. An irregularity in the rate of uptake or washout of the tagged substance may indicate an irregularity in biological functioning, such as that between normal and diabetic mice (Wolbarst 1993). The most glaring necessity for the probe or ligand in this case is to know the preferential organ uptake for comparison with pathological studies.

The essential characteristics of the necessary tags in such studies are complex. They should release primarily gamma radiation, they need to have a convenient half-life, and they need to be capable of detection outside the object (Wolbarst 1993). Also, the radionuclide needs to be readily attachable to the probe or ligand of interest in the biological study, and this attachment must be stable. It is helpful, but not necessary, for the gamma emission to be monochromatic such that scatter radiation can then be eliminated through energy windows (Wolbarst 1993). The collimator and electronic discrimination also serve to eliminate scattered radiation.

In our laboratory, we tag the agents with the radioactive isotope ^{125}I. Iodine has a half-life of 60 days, allowing it to be produced off-site and delivered by mail. Iodine's long half-life is also conducive to long-term storage and use, but it also means that injected radiation that is not excreted will not diminish as rapidly as some PET radiations, for example. Its principal radiation emissions are gamma rays (0.035 MeV and 6.5%), K$_{\alpha}$ X-rays (0.027 MeV and 112.7%), and K$_{\beta}$ X-rays (0.031 MeV and 25.4%) (Comar 1955). Although, the primary emissions of iodine-125 are not energetic enough for human

imaging research, the radiation energy is sufficient for small animal and phantom imaging. Our current SPECT studies use the iodine-125 in a NaI solution as a detection device only, injecting it within a phantom so that the x-rays and gamma radiation are "seen" by our gamma camera. No biological agent is used in these phantom studies.

In the future though, when we tag this iodine to other molecules/agents of interest, the radiopharmaceutical (agent and tag pair) will move by a process of active transport through the body of the animal being imaged, and it will become concentrated in particular parts of the body. For most iodine studies, any free iodine that might separate from the ligand becomes selectively concentrated in the thyroid, salivary, and gastric glands. It is excreted rapidly from the last two and retained for longer periods of time in the thyroid (Hobbie 1997). In fact, past radiation studies have shown that about thirty percent of the soluble radioiodine intake to the body can be assumed to accumulate in the thyroid of the subject (Comar 1955). This knowledge will help to distinguish interacting radiopharmaceuticals from separated and free iodine.

C. *Collimation*

The first part of the detector setup that the emitted radiation encounters is the collimator. A collimator is used in most tomographic applications to narrow the size of the beam striking the detector, thus reducing the amount of scattering photons detected. The collimator basically acts as a filter of the radiation. It is a block of absorbing material, usually lead or copper or some other high atomic number substance, with small holes drilled into its face, allowing only columns of light to pass through. The holes can also be chemically etched into the surface of thinner slices of collimator material that are

subsequently stacked and cemented together. The collimator thereby serves to confine the direction of incident photons and localizes the site of the emitter.

So that scattered photons do not interfere with the localization of the source, the collimator's walls must be just thick enough to block most of the photons that do not pass through the collimator holes and that directly contact its surface, or septa. In this way, the thickness of the collimating material plays a crucial role in the sensitivity of the results. Sensitivity here refers to the ratio of counts detected per unit time divided by the activity of the radioactive source; it is basically the count rate per unit activity (Weisenberger 1998). As the collimator thickness increases, the sensitivity decreases since fewer photons will reach the gamma camera. (It should be more readily apparent now why the electronic collimation of PET is a means to higher sensitivity. Since no external collimator is necessary for PET, more photons can be detected.)

The thickness of the collimator also has obvious repercussions with regards to resolution.[1] The more photons that are allowed to pass through the collimator to the detector, the more likely scattered photons are allowed to be detected and counted as emitted radiation. This can severely limit the minimum spatial resolution allowed by a detector system, for the resulting image will be blurred out by scattered photons. With a thicker collimator, the resolution of the image will increase, improving our results. For this reason, the collimator is sometimes termed the "eye" of the detector, as it is capable of focusing the incoming gamma radiation in this way.

Similar to the thickness of the collimator, both the direction of the holes in the collimator and the area of the apertures drilled or etched into the collimator face have

[1] See Appendix for a more concrete, mathematical examination of collimator and system resolution capabilities.

direct effects on the highest possible resolution and sensitivity achievable by one's detector system. The directional type of collimator most typically used in imaging applications is termed parallel-hole (and it is also the type of collimator used in these studies). In a parallel-hole collimator, all the apertures are parallel to one another. Yet, other similar studies may use pinhole collimators (magnifies or minifies objects depending on closeness of the camera), diverging collimators (minify objects), or converging collimators (magnify objects), each of which is pictured below in Figure 5 (Wolbarst 1993).

As is apparent, the diameter and depth of the holes limits the directional acceptance of the emitted photons. A photon not emitted in a direction corresponding to the orientation of the holes in the collimator will be absorbed by the collimator material (Saunders 2000). This directional limitation thus puts an additional ceiling on the possible sensitivity of the imaging system, but it can be used to improve resolution and subject contrast, just as with collimator thickness.

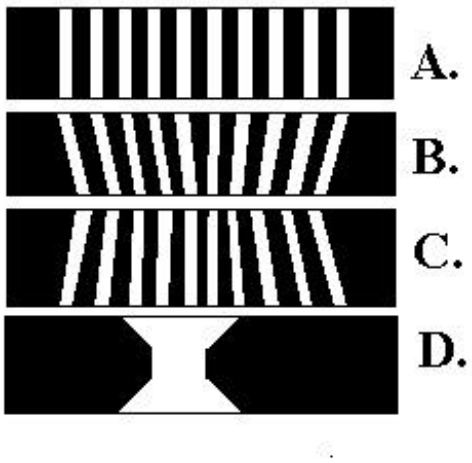

Figure 5 - A. Parallel-hole, B. Converging, C. Diverging, and D. Pinhole Collimators

In like fashion, the area of the aperture in the collimating material is also a parameter involved in the determination of system sensitivity and resolution. As the area of the aperture increases and more photons are allowed to pass through, the sensitivity of the detector goes up (Saunders 2000). As the aperture area decreases, fewer photons are allowed to pass, and thus fewer statistics are gathered and sensitivity decreases. Conversely, with a smaller aperture area, the detector system is able to resolve smaller areas of the emitting radiation. Thus, the resolution of the image increases with the decreasing aperture area. One notices the tradeoff that must be considered between sensitivity and resolution. In order to improve upon one aspect, one must sacrifice the other. The only solution is to the weigh the benefits of sensitivity versus resolution for each particular application of the technique being utilized. A final decision must be based upon the most important factors for that individual study.

For our purposes at the College of William and Mary, we have two separate collimators, both of which are copper-beryllium, parallel-hole collimators. They have been optimized for imaging of iodine-125 with a CsI(Na) crystal array with 1mm x 1mm crystal elements (Weisenberger 1998). Thermo Electron, of Woburn, MA designed both collimators, gluing together layers of copper-beryllium (approx. 1.9% Be) laminates. Photochemical techniques were used to construct square openings. One was designed as a high-resolution/low sensitivity collimator with 0.2mm openings and .05mm thick septa. The other collimator allows for increased sensitivity even though its resolution is not as high. This high sensitivity/low resolution collimator has 0.75mm openings with 0.16mm septa.

D. *Gamma Camera and Electronics*

After collimation, the next instrument encountered by the emitted radiation in the detection process is the gamma camera, or gamma-ray camera. The gamma camera was invented by Hal Anger in the late 1950's, and its purpose is to detect the photons emitted by the Iodine-125 (Cho 1993). The typical gamma camera is made up of an array of photomultiplier tubes with their entrance windows coupled to a large plate of crystal scintillator material by means of a light guide. Subsequently, they are sometimes referred to as scintillation cameras. The entire assembly is enclosed in a light-tight case that allows entry of the radiation.

Any radiation that makes it through the collimator first interacts in the crystal scintillator, producing a scintillation. A scintillator is a substance that absorbs radiation and produces visible photons with high efficiency, yet is transparent to them (Hobbie 1997). The scintillator works because the photons emitted by the radioactive iodine transfer some of their energy to atomic electrons in the scintillator through inelastic collisions, exciting the scintillation material. Some of the subsequent de-excitation then results in ultraviolet or visible photons. It is these visible photons that the phototubes detect in the next stage of the process. The photomultiplier tubes then give pulses providing information on the early location and time of the oncoming photon.

When the light flash strikes the photomultiplier tubes, electrons are emitted from the photocathode via the photoelectric effect. These electrons move through the vacuum of the photomultiplier tube, accelerating until they strike the surface of the first positively charged dynode. In a process called secondary emission, the kinetic energy that the accelerating electrons gain is sufficient to knock several electrons off the surface of the

dynode. The electrons that get knocked off the first dynode then accelerate to the next dynode, where the process, called electron multiplication, is repeated.[2]

Finally, once the end of the dynode chain has been reached, the electrons are collected by the crossed wire anode. The pulse of current striking the anode is proportional to the number of colliding electrons. Each current pulse at the output is called a count and is fed through discriminator electronics into ADC (analog-to-digital converter) cards that determine uniquely the size and location of the pulse, that is the amplitude and the x- and y-coordinates of each scintillation event on the scintillation crystal. Every count that is accumulated by the analog-to-digital converter cards is then recorded by a data accumulation program on a computer such that each count appears in an image according to its particular coordinates.

In the imaging setup that was designed for the detection of x-ray and gamma ray emissions of Iodine-125 in our laboratory, we have two available five-inch detectors. The two five-inch cameras are Hamamatsu R3292 Position Sensitive Photomultiplier Tubes (PSPMT's). The scintillator is composed of a CsI(Na) crystal array with 1mm x 1mm crystal elements that are 3mm thick. A 1 kV voltage is maintained between the photocathode and the last dynode of the PSPMT by a High Voltage Power Supply (Ortec Inc.). The detectors have 28 x 28 crossed wire anodes, but the number of output channels has been reduced by connecting anode wires in groups of two, creating a 14x X 14y channel readout. The entire assembly, as used in our lab, is depicted in a schematic cross section in Figure 6 on the next page.

[2] If there are n cascaded dynodes, and the average multiplication at each of the dynodes is m, then the overall charge multiplication of the dynode chain is m^n (Hobbie 1997).

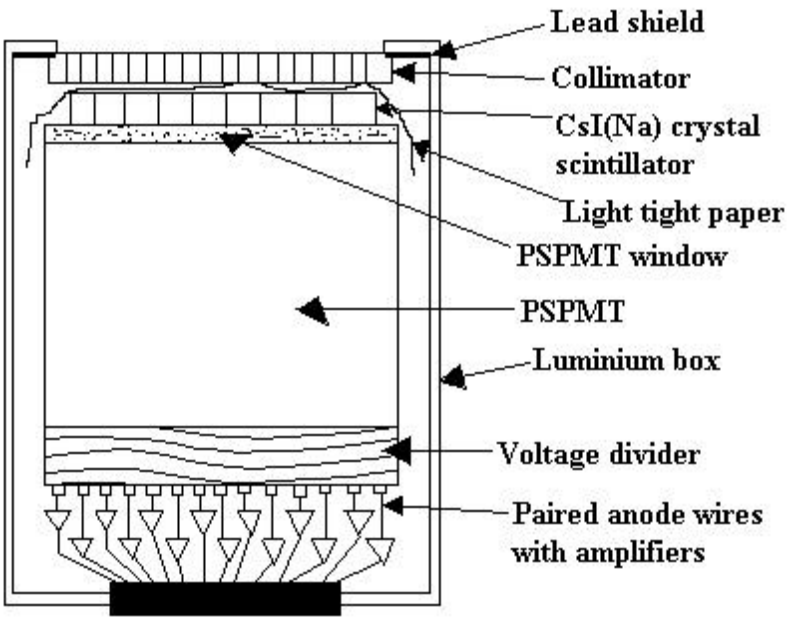

Figure 6 - Hamamatsu R3292 Position Sensitive Photomultiplier Tube

Both detectors are identical. The choice of which detector to use for which application comes from the type of collimator being used to "focus" the gamma radiation. The detector design allows for easy removal and replacement of collimator type. As mentioned, one collimator has narrower openings (0.2mm), providing a higher resolution but lower sensitivity. The detector using this collimator is termed the high-resolution detector (detector B). The other collimator has wider openings, at 0.75mm, for a more sensitive data accumulation. The detector with this collimator is our high-sensitivity/low-resolution detector (detector A).

In the configuration in our lab, the x- and y- outputs from each detector are separately fed into the analog-to-digital converter cards, which are located in the Sparrow CAMAC Crate Controller. The signal from the last dynode of the PSPMT is inverted and amplified prior to reaching the discriminator electronics so as to detect an event only if

the signal amplitude is above a predetermined background and noise threshold. The data from the CAMAC crate are fed to a G3 Macintosh Power PC workstation by SCSI cable lines. The Macintosh Power PC is our host computer, running all control software developed in the KMAX data acquisition system from Sparrow Corporation. The KMAX software, programmed as our data acquisition device, determines where each photon strikes the scintillator and excludes events that do not occur in a certain energy window. The window filters out lower energy radiation resulting from the primary gamma-ray Compton scattering in the phantom, the collimator, and the scintillator. The results are displayed as two-dimensional histograms on the G3 monitor in the KMAX applications software program.

E. *SPECT*

Up to this point, the detection scheme has consisted of concepts applicable to any gamma-ray imaging system and not particular to a study of SPECT; it is what has conventionally been called planar imaging, as the resulting image is just a two-dimensional or planar projection of the detected iodine from whichever angle the detector is facing with respect to the object or animal being studied. SPECT results are achieved by accumulating a number of these views, incrementally from 0° to 360°. Regardless of the number of views imaged and saved (so long as the total spans angles from 0° to 360°), the resulting images are then fed into the SPECT computer program. This program acquires all the data and returns a horizontal or vertical slice (depending on the orientation of the detectors) of the object being imaged. The horizontal or vertical slices

are then stacked to reconstruct the three-dimensional distribution of radioactivity within the subject.

Our computer program is based on the One Step Late algorithm invented by Peter Green and converted from C code to the IDL form we use by Dr. Steve Meikle of the Royal Prince Alfred Hospital in Sydney, Australia. It is a basic iterative procedure that compiles all of the acquired data, converts the incoming data to arrays, corrects each slice with a center of rotation offset, and displays a chosen slice of the object being imaged via backprojection. The program has been augmented to mask out unnecessary scatter radiation outside the region of interest that may corrupt the program. Also, all data entries with a value less than or equal to one have been converted to a value of one. This resolves any problems with zero in the calculation process and sidesteps any possible data underflow problems typical in SPECT outputs.

III. SPECT PHANTOM TESTS AND CALIBRATION

The research directed toward future small animal studies using SPECT has begun in our lab. We use a SPECT phantom and a centerline source to detect the radiation emitted by the injected iodine-125. Both phantoms are 3cm in diameter and 5cm in height. The centerline phantom has a 4cm long drilled tube running directly down its center for the injection of the radioactive iodine. The SPECT phantom has four drilled holes. The two vertical holes are 3.5cm long while the crisscrossed pair of holes are 2.75cm in length each. Both phantoms are depicted in Figure 7.

We have taken runs using these phantoms to assess the results of varying angular incrementing (small versus large), time duration of runs (short versus long), and choice of

detector usage (high resolution versus high statistics). These runs have been designed to test both the detector apparatus itself and the SPECT software used with this detector system.

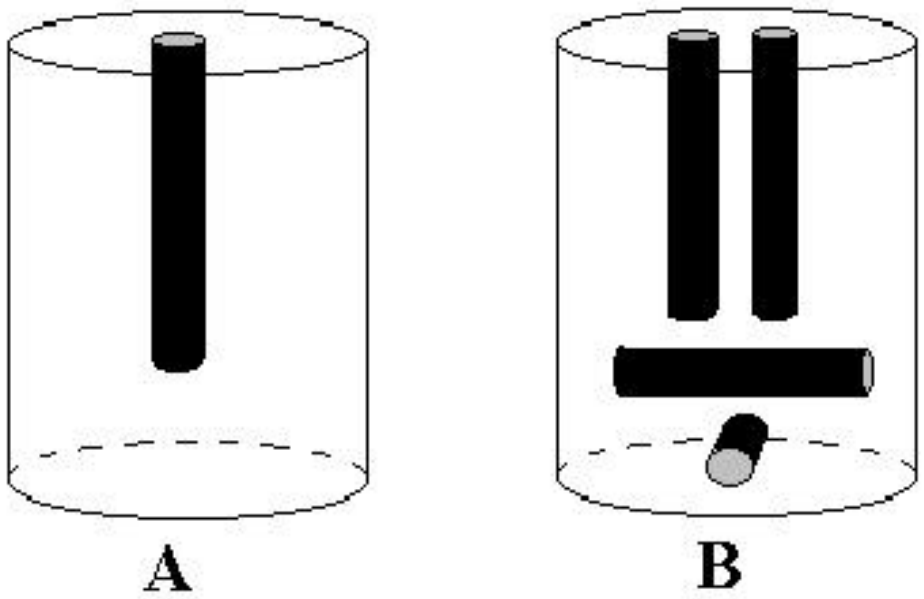

Figure 7 - A. Centerline Phantom and B. SPECT Phantom

The initial runs taken with this SPECT software were designed to test the trade-off between longer runs with larger angular increments and shorter duration runs with smaller angular increments. Smaller angular increments result in a larger amount of data accumulation because there are more runs overall. This should increase the number of statistics/counts gathered per run. However, shorter time for data accumulation also means that fewer counts will be recorded per angle. In the end, with the small increments and short duration, we will have more total angles imaged, but fewer statistics per angle. For the larger increments and longer duration, we will have fewer total angles imaged,

but more statistics acquired per angle. Each run should acquire a relatively equal amount of *total* data. In this way, we can compare the SPECT results considering these differing combinations and similar amounts of data accumulation.

Four runs were made with the above phantoms. The high-resolution detector (detector B) was used for all of the data accumulation. In general, the gamma camera scans linearly along the phantom at a given view θ, and after completion of this scan, the source phantom is rotated through an angle $\Delta\theta$. The process is repeated until the completion of the 360°-rotation, resulting in a total of $360/\Delta\theta = N$ scans per run.

The first run imaged the centerline phantom, which would subsequently be used in each of the next three runs as a center of rotation (COR) correction in the SPECT calculations. Great care had to be taken to ensure that the base designed to rotate the phantom was not disturbed or shifted from its initial position. Any disturbance of the location of the center of rotation affects COR offset calculations in the SPECT program. We placed the centerline phantom a few millimeters away from the detector, just far enough so that rotating the phantom would not disturb its center of rotation[3]. This COR run consisted of 10 incremental views, each separated 36° from the previous angle and lasting three minutes in duration. For example, we started at 0°, collected data in KMAX for three minutes, rotated the phantom 36°, collected data once again, etc. all the way up to 324° (360° – 36°). The 360° angle is not necessary since it coincides with 0°. If both angles are imaged, the SPECT program just ignores one of them. The centerline run does not need to be as thorough as the runs with the actual SPECT phantom, so not as much data acquisition time is necessary.

[3] Closer objects are imaged at a higher resolution than farther ones. See Appendix.

The second, third, and fourth runs were all done using the SPECT phantom, again placed only a few millimeters away from the high-resolution detector, as depicted below in Figure 8. The second run used 6° increments and a three-minute data collection duration. The third run used 12° increments and six minutes per angular view, while the fourth run tested 24° increments with twelve minutes allowed for data accumulation. A summary of these runs, along with the other runs taken for our SPECT testing, is depicted on the next page in Table 1.

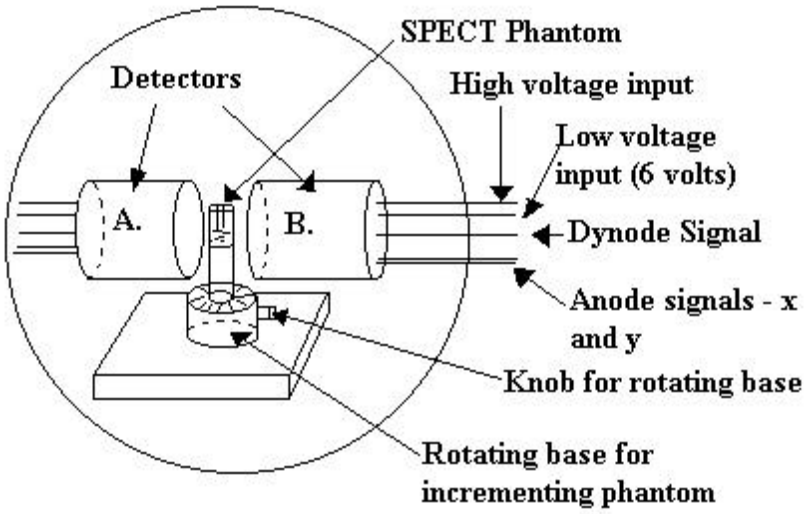

Figure 8 - The SPECT detector configuration in our lab. Both detectors, A and B, are aligned horizontally to image the phantom of interest, which is placed as close as possible to each detector. The rotating base is used to increment the phantom through successive angular degrees, allowing the accumulation of a sufficient collection of projections for the SPECT computer program.

Each run has its own folder to be opened and run through the SPECT software program. Each individual image is saved in KMAX according to its particular angle and stored in the folder for its run. The SPECT computer program then retrieves the folder, converts each KMAX image histogram into a two dimensional data array, masks out scattered counts, and returns an image of the desired slice of the phantom.

The same general procedure was repeated again for additional data. This time we used both detectors simultaneously to compare results between high-resolution and high-statistics detection. The centerline phantom was again used to correct for COR offsets. This run, Run 5, was formatted identical to the initial centerline study. We used 36° increments with three-minute data accumulation. The results for the imaging of the phantom were stored separately for each detector. We used the same SPECT phantom as before for our 6th Run, placing it equidistant between the two detectors and no more than a few millimeters from either. A three-degree increment was used this time, and we imaged each angular view for three minutes. The same means of data storage and analysis were used on this accumulation of images. A summary of the runs that were taken is illustrated below in table format, Table 1.

Run	Phantom Used	Detector A	Detector B	Time duration	Angular increment
1	Centerline	No	Yes	3 minutes	36°
2	SPECT	No	Yes	3 minutes	6°
3	SPECT	No	Yes	6 minutes	12°
4	SPECT	No	Yes	12 minutes	24°
5	Centerline	Yes	Yes	3 minutes	36°
6	SPECT	Yes	Yes	3 minutes	3°

Table 1

IV. RESULTS

The aim of this project has been to test our detector system to see if the existing set-up could be configured properly to acquire SPECT data. We have acquired all of the necessary data and hope to have it analyzed in the near future. The next step of the process will be to successfully run the data through our SPECT software to recreate sliced images of the iodine-125 injected in the SPECT phantom. The data, as acquired in our KMAX data accumulation program, initially looks like that depicted below in Figure 9 below.

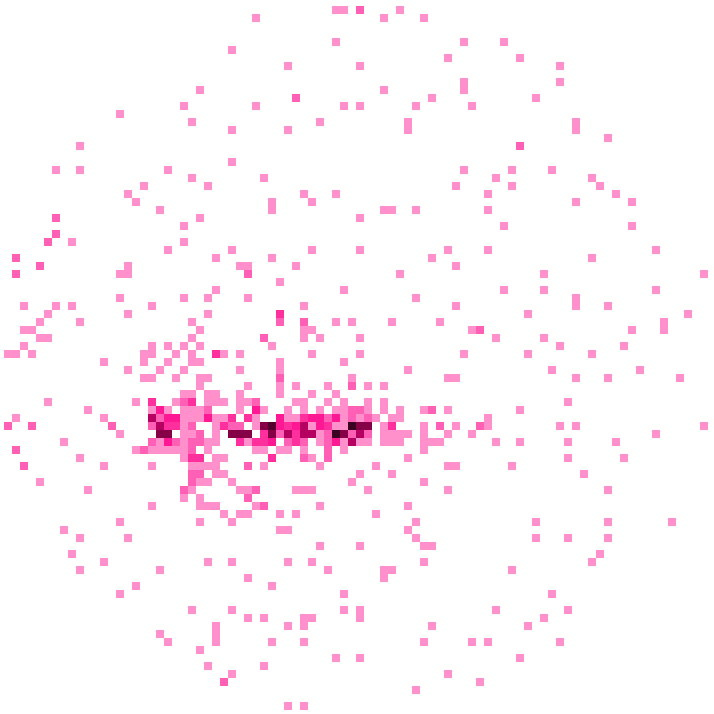

The detected radiation forms a circular image inside the square KMAX data acquisition window. This particular image depicts the radiation emitted from the SPECT phantom that was accumulated at an angle of 240° using the high-resolution detector (detector B) for a three-minute duration (Run 2). Each detected count of radiation appears as a point on the data accumulation screen, and the majority of the data points are concentrated around the areas of the tubular holes bored in the SPECT phantom, where the iodine was injected.

The conclusions that we have made based on the data that was accumulated in these runs are twofold: 1) The amount of total statistics is a crucial factor in the ability of the SPECT software to compile and run the data, as the SPECT program is extremely sensitive to the amount of data accumulation. The factors involved in the number of acquired statistics include both the number of angular increments and the time duration per angle, as well as the amount of radiation emitting from the radioactive iodine per unit time, i.e. the hotness of the phantom. With this in mind, the SPECT phantom needs to be recharged before each run and evenly dispersed throughout the entire length of each of the tubes in the phantoms. Recharging the phantoms ensures that the maximum amount of statistics will be gathered per phantom per run. Equally dispersing the radiation through the tubes further aids in the maximal utilization of the radiation injected within the phantom. A similar consideration regarding the amount of statistics is that the SPECT program prefers to see a larger number of angles such that the angular increments are small. And the program wants long time durations for each angular increment, both of which increase the amount of data accumulation. Once the data from Runs 1 through 4 can be successfully run through our SPECT program, it will be apparent which factors

weigh more heavily. 2) The orientation of the detectors in the acquisition phase play a crucial role in the ability of the SPECT program to properly correct for the center of rotation offset. The convention is that the axis of rotation projects onto a vertical line in the center of the two-dimensional data array at each angle. The data that were accumulated in all of our runs were projected horizontally in our KMAX software, so the center of rotation (COR) offset revolves around the opposite axis as that of our COR correction data.

On top of needing to recharge the phantoms with the necessary iodine-125, running the program made it clear that changes needed to be made in the computer code itself. Floating point underflow error messages illustrated the fact that the program was not properly reading the data. Absolutely no images were being produced at all. To counter the floating underflow problem, the program was corrected to convert all negative and zero data points to a value of one. This was done manually in the computer code. Additionally, the outer lying scattered radiation reaching the detectors was masked out of the data that we fed into the SPECT program to compile and run the software. The masking factor is a changeable parameter in our SPECT program that cuts out the slices of the image outside of the region of interest. This allows for the program to ignore those regions of the image with lower statistics than the regions of radioactive emissions.

The mask that we used to hide data is illustrated on the next page in the accumulated KMAX image of Figure 10. This image was taken using our high-statistics detector (detector A). It depicts the SPECT phantom at an angle of 240° after a three-minute duration. Because the KMAX image is a square, while the detected radiation from the gamma camera forms a circular region of detected radiation, areas outside the

circle return a value of zero to the data analysis program. Additionally, very few counts are detected outside the region directly surrounding the injected radiation. The lack of data in both these regions was causing the floating-point underflow problems, so the implemented mask "hides" these regions of low data and forms a window around the region of interest including and directly surrounding the injected radiation.

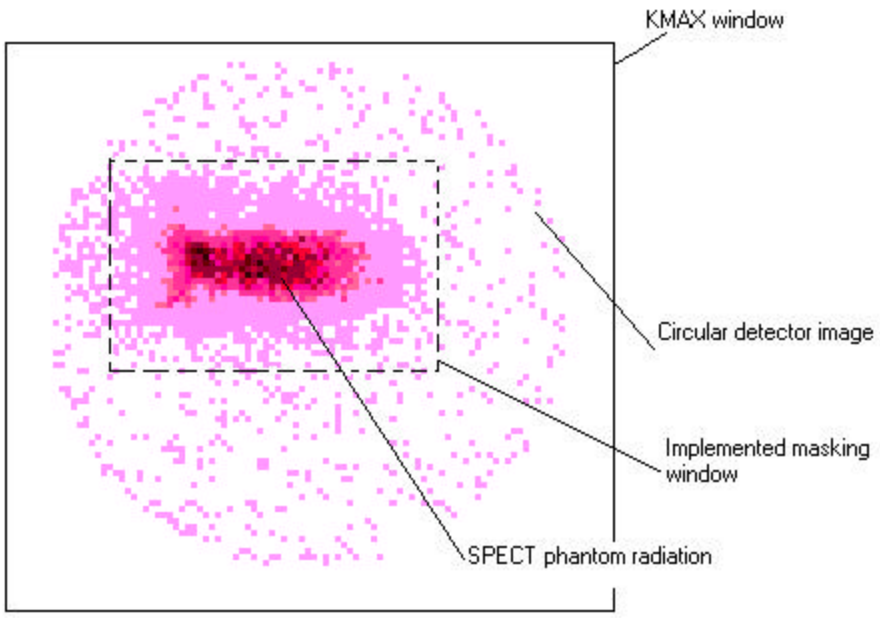

Figure 10 - Masking of acquired data.

The runs designed to test the capabilities of the high-resolution detector versus the high-statistics detector – Runs 5 and 6 – were successful. The two phantoms were recharged with iodine-125 solution in hopes of acquiring more total data with our low statistics detector B. The high statistics detector A was used as a comparison in resolution and counts acquired per angle. Two typical accumulated KMAX images have been depicted on the next page in Figure 11 and Figure 12. Figure 11 shows the statistical results of detector A while Figure 12 shows the results from detector B.

Figure 11 - Centerline phantom using detector A.

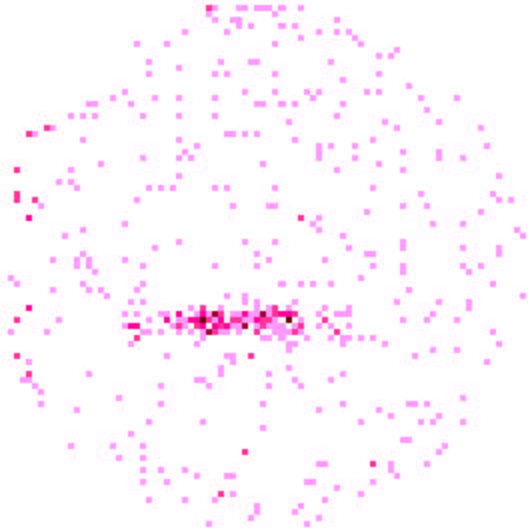

Figure 12 - Centerline phantom using detector B.

Both images were formed in Run 5 by the respective detector for three-minute simultaneous data accumulation using the centerline phantom. The disparity in resolution and the difference in statistical accumulation for the corresponding detectors are readily

apparent in comparing the two images. Detector A's image, in Figure 11, has a larger amount of acquired counts but the resolution is much worse that that of detector B in Figure 12.

The conclusions derived from these runs showed us that the orientation of the detectors upon imaging plays a crucial role in the ability of the SPECT program to correct for the center of rotation offset. In Figures 11 and 12, for instance, one can see that the planar images in KMAX project horizontally rather than vertically; however, the program prefers a vertical orientation of the image. Rotating the KMAX images ninety degrees before running the program will project the data on the vertical axis so that the program will recognize the image format. The resulting image should look like the following, in Figure 13 below, which is a rotated depiction of Figure 11. To avoid this complication in the future, data should be taken with the detectors oriented for vertical projection.

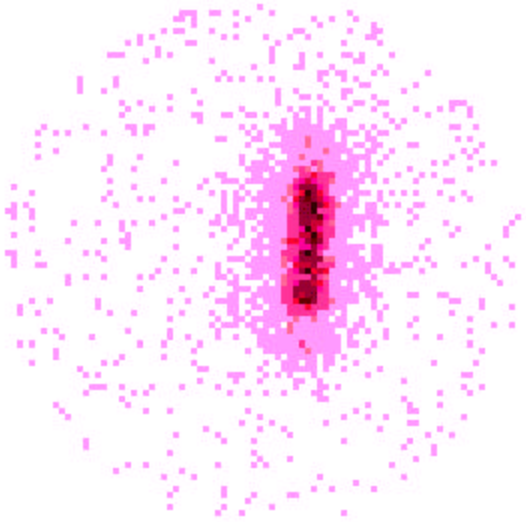

Figure 13 - Rotated image of horizontal planar image. Rotation of the image by ninety degrees orients the image vertically so that the data analysis software program can recognize the format.

Overall, the fact that we were able to run the data through the SPECT program in order to pinpoint the problems involved showed that the detector set-up has the capabilities necessary for SPECT runs. The SPECT images, to this point however, have been used mainly as a means of uncovering program malfunctions rather than as a correct depiction of sliced images of radiation from our phantoms. The majority of our sliced images of radiation have the general format of one of the two images below.

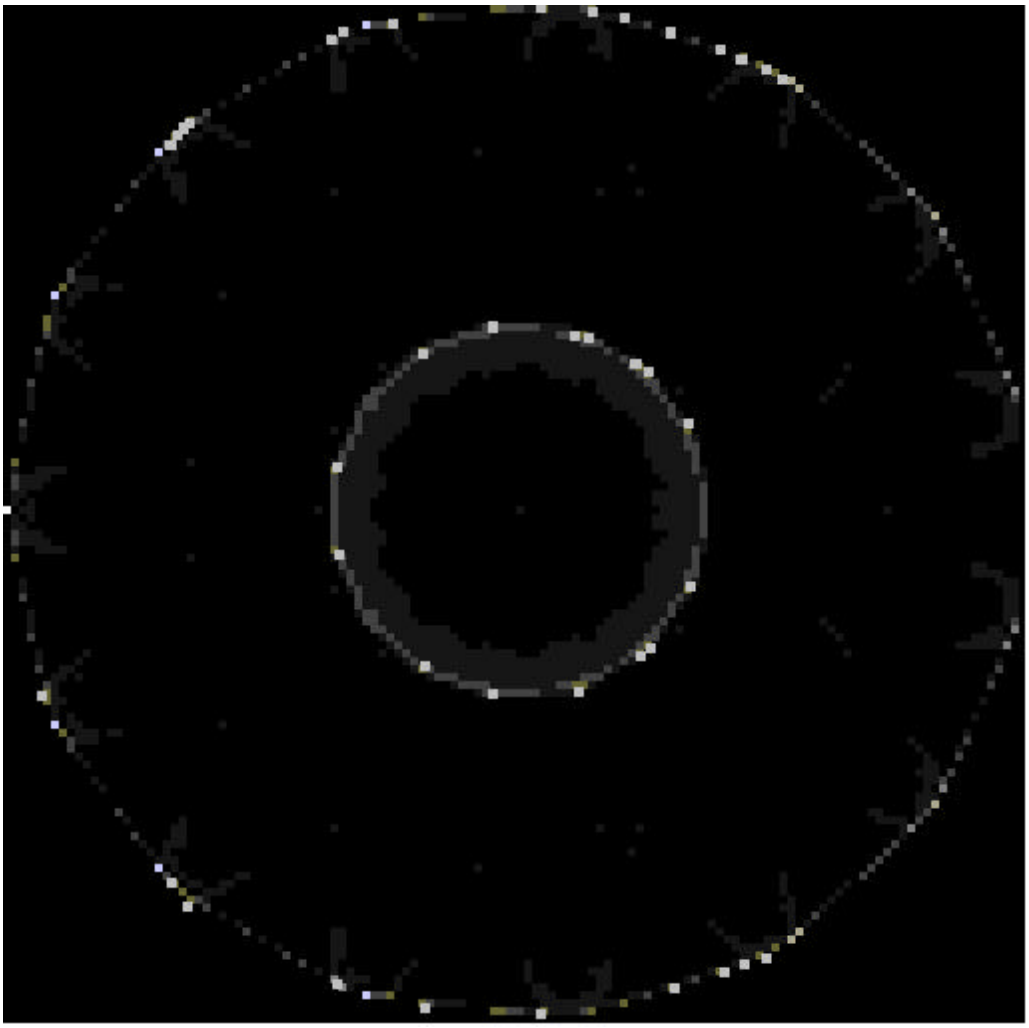

Figure 14 - SPECT image of slice 45 from Run 2.

Figure 15 - SPECT image of slice 50 from Run 2.

Figures 14 and 15 both tend to show a failure to correctly adjust for the center of rotation. Figure 14 depicts two concentric circles while Figure 15 has a whirlpool-like formation of data points toward its center. Both figures have aided in targeting our problems with the centerline correction and the orientation of the detectors.

The lack of SPECT results to this point basically rests in the program's inability to recognize the format of our rotated images. The program is specific to the format of the KMAX images, so even though all the data have been acquired and saved successfully, SPECT results cannot be achieved. Further reparations in the SPECT

program and in the method of data acquisition will help promote the ability to achieve results in the sliced image display. The data that have been taken in Runs 1-6 can then be utilized to test the parameters of the detector system that they were designed to analyze.

V. APPENDIX

A. *Resolution determination for a parallel-hole collimator*

The resolution of a parallel-hole collimator can be determined by the following equations (Weisenberger 1998):

$$R_C = d (a_e + b + c) / a_e \quad (1)$$

$$a_e = a - 2/\mu \quad (2)$$

where

R_C = collimator resolution

d = aperture size

a = collimator thickness

a_e = effective collimator thickness

μ = linear attenuation coefficient of collimator material at energy of gamma rays

b = distance between the source and the collimator face, and

c = distance between the back of the collimator and the front of the scintillator

B. *System resolution*

The system resolution is determined from both the resolution of the collimator and the intrinsic resolution of the detector. The inherent resolution of the detector is set as the pixel size of the scintillator, or 1 mm for our studies. In general, the intrinsic resolution of the detector is the ability of the camera to pinpoint the location at which incoming photons interact on the scintillation crystal (Cho 1993). Basically, the more photomultiplier tubes present in the detector, the better its intrinsic position resolving

capability. Probability and statistical fluctuations set the limit on how high the intrinsic resolution can be. The overall system resolution is then:

$$R_S = (R_C + R_i)^{1/2} \quad (3)$$

where R_i = the intrinsic resolution of the gamma camera (Weisenberger 1998). Typically, the resolution of the collimator can be a much larger contributor to overall system resolving capabilities.

VI. ACKNOWLEDGMENTS

Many people have been influential in the completion of this research. Each of these people helped me in their own way in finishing this study and understanding it. For that, I am grateful. Most of all, great appreciation and thanks go to Dr. Robert E. Welsh, my advisor, mentor, and motivator. Additional thanks and awe go out to Dr. Drew Weisenberger, who helped to design the detector system used in our laboratory. I cannot even imagine the time that had to be spent to start from scratch and design this equipment and procedure. I would also like to thank Dr. Steve Meikle for his help and consideration concerning the SPECT computer code used in our lab. His correspondence throughout my project has been of considerable generosity and invaluable help. Rob Saunders and John Feldmann, both students working on this project with me in some aspect, have also been a vast help. Without John and Rob, I would not understand either the method of data acquisition in our lab or the means to analyze this data with our computers. I happily acknowledge the time that they spent to help me understand this project. A special thanks goes to the Howard Hughes Medical Institute for awarding me with the Student Research Grant for this project. And of course, thanks go to my parents, brother, teammates, and friends, for always supporting me and helping me get through whatever obstacles have come up on my journey through college.

VII. BIBLIOGRAPHY

Chandra, Ramesh. Introductory Physics of Nuclear Medicine, pp. 57-70, Lea & Febiger, Philadelphia, 1976.

Cho, Z.H., Jones, J.P., and Singh, M. Foundations of Medical Imaging. pp. 148-233, John Wiley and Sons, New York, 1993.

Comar, C.L. Radioisotopes in Biology and Agriculture, McGraw-Hill, New York, 1955.

Herman, G. T. Image Reconstruction from Projections: The Fundamentals of Computerized Tomography, pp. 1-25, Academic, New York, 1980.

Hobbie, R. Intermediate Physics for Medicine and Biology, 3rd ed., pp. 417-491, Springer, New York, 1997.

Pullan, B. R. "Basic Principles of Computed Tomography: Theory." *Proceedings of the International School of Physics: <<Enrico Fermi>>*, Course LXXVI, pp. 20-33, North Holland Publishing Co., Amsterdam, 1981.

Robb, R. A. Three Dimensional Biomedical Imaging, pp. 21-72, VCH Publishers, New York, 1995.

Saunders, R. "Development of a Gamma Camera Array for Biological Imaging in Small Animal Research," Undergraduate Thesis, College of William and Mary, Williamsburg, VA, 2000.

Shepp, L. A. "Computed Tomography." *Proceedings of Symposia in Applied Mathematics*, vol. 27, pp. xi, AMS, Providence, 1983.

Weisenberger, A. "Gamma-ray Imaging Detector for Small Animal Research," Doctoral Thesis, College of William and Mary, Williamsburg, VA, 1998.

Wolbarst, A.B. Physics of Radiology. pp. 299-360, Appleton & Lange, Norwalk, 1993.